The Cryosphere Discuss., 8, 3999–4031, 2014
www.the-cryosphere-discuss.net/8/3999/2014/
doi:10.5194/tcd-8-3999-2014

The Cryosphere
Discussions
Open Access

Wintertime storage of water in buried supraglacial lakes across the Greenland Ice Sheet

L. S. Koenig[1], D. J. Lampkin[2], L. N. Montgomery[2], S. L. Hamilton[3], J. B. Turrin[4], C. A. Joseph[2], S. E. Moutsafa[5], B. Panzer[6], K. A. Casey[7,1], J. D. Paden[6], C. Leuschen[6], and P. Gogineni[6]

[1]Cryospheric Sciences Laboratory, NASA Goddard Space Flight Center, Greenbelt, MD, USA
[2]Department of Atmospheric and Oceanic Sciences, University of Maryland, College Park, MD, USA
[3]Bowdoin College, Brunswick, ME, USA
[4]Department of Geography, University of Utah, Salt Lake City, UT, USA
[5]Department of Geography, Rutgers, The State University of New Jersey, Piscataway, NJ, USA
[6]Center for Remote Sensing of Ice Sheets, University of Kansas, Lawrence, KS, USA
[7]Earth System Science Interdisciplinary Center, University of Maryland, College Park, MD, USA

Received: 26 June 2014 – Accepted: 1 July 2014 – Published: 18 July 2014

Correspondence to: L. S. Koenig (lora.s.koenig@nasa.gov)

Published by Copernicus Publications on behalf of the European Geosciences Union.

Abstract

Surface melt over the Greenland Ice Sheet (GrIS) is increasing and estimated to account for half or more of the total mass loss. Little, however, is known about the hydrologic pathways that route surface melt within the ice sheet. In this study, we present over-winter storage of water in buried supraglacial lakes as one hydrologic pathway for surface melt, referred to as buried lakes. Airborne radar echograms are used to detect the buried lakes that are distributed extensively around the margin of the GrIS. The subsurface water can persist through multiple winters and is, on average, $\sim 4.2 + 0.4$ m below the surface. The few buried lakes that are visible at the surface of the GrIS have a unique visible signature associated with a darker blue color where subsurface water is located. The volume of retained water in the buried lakes is likely insignificant compared to the total mass loss from the GrIS but the water will have important implications locally for the development of the englacial hydrologic network, ice temperature profiles and glacial dynamics. The buried lakes represent a small but year-round source of meltwater in the GrIS hydrologic system.

1 Introduction

Annual mass loss from the Greenland Ice Sheet (GrIS) has substantially increased, quadrupling, in the last two decades (Shepherd et al., 2012). Surface melt over the GrIS is estimated to account for half or more of the total mass loss (van den Broeke et al., 2009; Enderlin et al., 2014) as calculated from models using a rudimentary physical treatment of the complex hydrologic system. With this increasing GrIS surface melt, the englacial pathways the meltwater and runoff flow through are still relatively unknown, unquantified and not simulated in surface mass balance models (Rennermalm et al., 2013). Understanding englacial storage and routing is of increasing importance as GrIS surface melt increases with rising Arctic temperatures (Comiso, 2003), highlighted by a record melt event in 2012 (Nghiem et al., 2012; Hall et al., 2013; Hanna et al., 2012).

Regional climate models, that agree relatively well (~ 20 % variation) on precipitation amounts across the GrIS, still have large discrepancy (from 38–83 % variance) in melt production, refreeze, and runoff (Vernon et al., 2013). Recent field observations and models of water retention and latent heating from refreeze on the perimeter of the GrIS punctuate that englacial water routing and storage can cause significant warming to the ice that must be captured to accurately model runoff (Forster et al., 2013; Koenig et al., 2014; Harper et al., 2012; Kuipers Munneke et al., 2014; Humpherys et al., 2012). The uncertainties in englacial storage and routing must be reduced in order to improve projections of future sea level rise (SLR) (Rennermalm et al., 2013).

This paper presents a previously unmapped hydrologic pathway for surface melt retention within the GrIS in buried supraglacial lakes. Referred to here as a buried lake and defined as water at shallow depths in the ice sheet that was previously a supraglacial lake and currently exists under lake ice and, in most instances, under a snow/firn layer. Here we present near-surface, high resolution radar data, collected during the Arctic Spring Campaigns of Operation IceBridge (OIB), that clearly show water retention in buried lakes through the winter season illustrated by Fig. 1. This water represents a latent heat source (Humphreys et al., 2012; Kuiper Munneke et al., 2014) currently unaccounted for throughout the winter as well as a mechanism for propagating cracks or moulins (Das et al., 2008) providing further evidence that the englacial hydrologic system remains active even during the cold winter months (Rennermalm et al., 2013).

2 Background

Several have studied supraglacial lakes, which are easily distinguishable by visible satellite, when they form seasonally in the ablation and percolation zones across all geographic regions of the GrIS (Echelmeyer et. al., 1991; Box and Ski, 2007; McMillan et al., 2007; Sneed and Hamilton, 2007; Sundal et al., 2009; Lampkin, 2011; Selmes et al., 2011; Tedesco and Steiner, 2011; Howat et al., 2013). Supraglacial lakes form in local topographic lows formed by bedrock depressions, which are not advected by the ice and often reform in the same locations (Echelmeyer et al., 1991; Box and Ski, 2007; Selmes et al., 2011). Das et al. (2008) observed the drainage of a supraglacial lake through fractures, rapidly (< 2 h) delivering surface meltwater to the bedrock–ice interface resulting in local uplift and acceleration through hydro-fracture (van der Veen et al., 1998; Alley et al., 2005; van der Veen, 2007; Krawczynski et al., 2009). The englacial network of conduits formed from lake drainages, as well as surface crevasses filled with water, provides pathways for surface meltwater to reach the bed of the GrIS, thus causing a dynamical increase to some threshold value, in ice velocity towards the sea (Zwally et al., 2002; Joughin et al., 2008; Catania et al., 2008; Bartholomew et al., 2011; Palmer et al., 2011; Sundal et al., 2011; Hoffman et al., 2011; Tedstone et al., 2013).

Most studies have assumed that supraglacial lakes either drain during the summer or refreeze during the winter. Ohmura et al. (1991) did observe evidence of persistent water in lakes by the presence of ice plates on the surface at West Lake near Swiss Camp in Western Greenland. Additionally, they detected a deep lake (∼ 10 m) to the east of Swiss Camp that likely remained water filled through the winter developing lake ice up to 1.5 m thick before draining in spring or early summer. Rennermalm et al. (2013) also showed evidence of water retention of up to 6 months from peaks in stream discharge that occurred in the absence of surface melt in the fall and spring. There has not been a systematic assessment of the extensive high-resolution radar data (first provided by OIB in 2009) to confirm wintertime storage of water in supraglacial lakes or to map the spatial and temporal distribution. This effort, therefore, is the first to characterize wintertime meltwater storage in buried lakes over the GrIS and provide a first-order assessment of it impact on hydrology.

3 Data

3.1 Radar data

Radar backscatter data acquired from the CReSIS ultra-wideband Snow Radar (Leuschen, 2014) during OIB Arctic Campaigns from 2009 through 2012 are used to identify subsurface water. The radar operates over the frequency range from ~ 2 to 6.5 GHz where water has a high absorption coefficient resulting in the attenuation of radar waves and a strong reflection of the wave at the ice–water interface due to the large difference between the dielectric constant of ice and water (Fig. 2) (Ulaby et al., 1981). The Snow Radar uses a Frequency Modulated Continuous Wave (FMCW) design which provides a vertical resolution of ~ 4 cm in snow/firn to a depth of tens of meters. Radar backscatter along a transect is often displayed as an echogram (Fig. 2) which provides a visual image of the subsurface returns. For additional details on the Snow Radar performance see Panzer et al. (2013) and Rodriguez-Morales et al. (2014).

3.2 Visible imagery

Visible imagery is used from several imaging platforms to support the analysis of buried lakes. OIB Digital Mapping System (DMS) imagery, acquired coincident with Snow Radar data, is used to examine surface features indicative of the presence of subsurface water. Cloud-free Moderate Resolution Imaging Spectroradiometer (MODIS) Rapid Response Arctic Subset true color imagery (250 m resolution) was used to determine if supraglacial lakes formed previously at the location of the buried lakes. Additionally, at a sample lake site, MODIS Land Surface Temperature (LST) data are used to corroborate melt onset and surface thermal conditions along with Landsat, Enhanced Thematic Mapper (ETM+) panchromatic imagery, with a resolution of ~ 15 m, to evaluate the summertime evolution of the lake.

DMS acquires imagery in the visible part of the electromagnetic spectrum at a nominal resolution of 10 cm (at 1500 feet AGL, the nominal OIB flight altitude). DMS collects data over three multispectral and panchromatic bands using a 21 megapixel Canon EOS 5D Mark II digital camera. Data are orthorectified and corrected for camera orientation using the Applanix POS/AV navigation system. For additional details see Dominguez (2014).

MODIS LST (MOD11A1, version 5.1) swath data at 1 km resolution over a sample lake region were used in this analysis. MODIS LST, over snow and ice, are accurate to within ±1 °C (Wan et al., 2002; Hall et al., 2008) for ice surface temperatures between −15 to 0 °C (Hall et al., 2008). MODIS LSTs acquired over GrIS, however, can be ∼ 1 to 3 °C colder than the actual surface temperatures (Hall et al., 2013; Koenig and Hall, 2010).

4 Methods

4.1 Detection of buried lakes from airborne radar

All Snow Radar echograms over the GrIS from 2009–2012 were manually inspected for subsurface attenuations of the radar backscatter, possibly attributed to a buried lake (Fig. 2b). To ensure the radar response was associated with englacial water, and not some other density or dielectric change, all 2011 detections from Snow Radar data were compared to either the Accumulation Radar (∼ 600–900 MHz) or MCoRDS Radar (∼ 140–260 MHz), flown simultaneously with the Snow Radar onboard the OIB aircraft (Fig. 2). Water attenuates across radar frequencies. If at least one additional radar showed attenuated backscatter the detection remained in the dataset. Additionally, all detections were compared to summertime cloud-free MODIS imagery to confirm that a supraglacial lake formed at the buried lakes location during a melt season (Fig. 3). The 2011 Snow Radar data were chosen for this initial analysis because it was the first

TCD
8, 3999–4031, 2014

year in which the OIB radar operators discovered the unique return over supraglacial lake regions.

The analysis of the 2011 Snow Radar data lead to two characteristic echogram patterns for englacial water retention: buried supraglacial lakes (Fig. 2b) and water-filled crevasse fields (Fig. 4). The water-filled crevasse fields were not included in the analysis presented here because, though it is likely they contain englacial water, it is also possible that the crevasses, or hoar crystals formed within them, are scattering the radar signal causing a similar backscatter signature to subsurface water. Additional field verification is needed to confidently interpret radar backscatter over crevassed regions.

The buried lake detections from 2011 were mapped using approximately the center point of the feature and were compared to high resolution (cm-scale) DMS imagery of the GrIS surface coincident with the radar collection (Fig. 5) (Dominguez, 2014). DMS imagery is used to visually characterize the surface roughness, detect crevasses and to look for any distinct surface expression of the buried lakes.

Finally, to construct a time series of buried lakes, the characteristic buried-lake radar return Fig. 2b), determined from the 2011 data, were used to map buried lakes from the 2009, 2010 and 2012 Snow Radar data. Buried lakes that formed within 1 km of each other from year-to-year are considered the same feature. Selmes et al. (2011) reported a median area of 0.56 km^2 and a mean area of 0.80 km^2 for lakes across the GrIS. Because the buried lakes were mapped using an approximate center point, a 1 km radius is a reasonable distance to be considered the same feature along the changing OIB flight lines.

4.2 Depth retrieval of the water surface

The 2011 Snow Radar echograms of the buried lakes were manually digitized to determine the depth from the snow surface to the water surface. If distinguishable in the echogram, as shown in Fig. 2b, both the snow-lake ice interface and the lake ice–water interface were digitized. When a snow layer is digitized, a constant density of

320 kg m^{-3}, a reasonable density estimate for the top meters of snow across the GrIS (Benson, 1962), is used to convert radar travel time to depth using equations developed by Wiesmann and Matzler (1999). When a lake ice layer is digitized or if only the snow surface and the water layer are digitized, the dielectric properties of ice are assumed to convert radar travel time to depth (Dowdeswell and Evan, 2004). In the absence of field data providing a stratigraphic density profile, the ice assumption is made which biases the depth measurements to shallower depths. The uncertainties in the depth are estimated by taking the subset of radar echograms where a snow layer was detected and calculating the depth with both the snow layer and ice assumptions. The average percent difference defines the uncertainty at 10 % (range of 2 % to 22 %) shallower because radar waves travel slower in solid ice than snow/firn which contains more air.

5 Results

5.1 Spatial and temporal distribution of buried lakes

The wintertime storage of meltwater in buried lakes is extensive around the margin of the GrIS (Fig. 6). All buried lakes identified from 2009–2012 were below the 2000 m contour of the GrIS with the majority falling between 1000 m and 2000 m on the west coast of the ice sheet (Fig. 6). Table 1 provides the number of buried lakes detected each year, the mean and standard deviation of buried lake elevation, the number of buried lakes below 1000 m and the distance of OIB flight lines flown below 2000 m. Because OIB is an airborne mission with a changing set of flight lines leading to an inconsistent spatial sampling, temporal changes in the detection and elevations of buried lakes cannot be assessed and quantified directly. In Table 1, however, it is clear that the more distance flown below 2000 m leads to more detections of buried lakes.

Clusters of buried lakes are concentrated along the west coast of Greenland and near 79° N and Zashariæ Isstrøm Glaciers where OIB gridded flight lines are flown re-

TCD
8, 3999–4031, 2014

peatedly in multiple years (Fig. 6). It is also in these regions where we detect buried lakes that persist for multiple years (Fig. 7). Again, these multi-year detections must be taken in context, they occur in areas with high concentrations of supraglacial lakes where OIB flightlines were repeated in multiple years. It is very likely that other buried lakes are present through multiple winters that are not being detected due to the limited OIB spatial sampling. Table 2 list the number of occurrences of repeat detections between any two years. In addition, 7 lakes were detected in 3 of the 4 years (Fig. 7). All lakes detected over three seasons were located on the OIB grid near Jakoshavn Isbræ repeated annually.

5.2 Surface expression of buried lakes and lake evolution

DMS imagery rarely shows any surface expression of the buried lake (Fig. 5). At five locations, however, a unique surface expression was found when the buried lake's ice covered surface was exposed (examples from three of the buried lakes shown in Figs. 5, 8 and 9). These figures show relatively darker blue ice adjacent to a region of lighter colored ice indicating a transitional zone in subsurface conditions revealed in radar echograms (Figs. 5 and 8). While scattering and absorption of visible light over buried lakes is indeed complex with snow, water, lake ice and glacial ice (Grenfell and Perovich, 1981; Warren, 1984), the darker blue color associated with retained water can be explained by the vibrational transitions as well as the higher density and temperature of water molecules in the buried lake liquid water resulting in stronger hydrogen-oxygen bond absorption feature near 600 nm. Simply, the hydrogen bonds in liquid water cause a shift to lower energy over ice which would produce the darker blue color (Luck, 1980; Langford et al., 2001). Figure 8 shows a high resolution example of a buried lake, detected on 2 May 2011 approximately 50 km inland from the terminus of Zachariae Isstrøm Glacier in Northern Greenland, with a surface expression that provides information about the lake's evolution. Figure 8 shows blowing snow across the clear frozen surface of the lake ice, water filled cracks on the lake bed, a pressure ridge, likely caused by displacement of bouyant ice over subsurface water adjacent to

TCD
8, 3999–4031, 2014

Wintertime storage of water in buried supraglacial lakes across the GrIS

L. S. Koenig et al.

static ice, and the characteristic darker blue color of the region with retained water. Figure 8 also shows polygonal regions of ice that were likely floating lake ice refrozen into the newly formed lake ice. This suggests that the lake ice never completely thawed from the previous melt season and that this lake has persisted for at least two winters.

Figure 9 shows a radar echogram and DMS image of another lake detected on 2 May 2011, approximately 100 km inland from the terminus of 79°N Glacier in Northern Greenland. Radar backscatter clearly shows melt on the surface (Fig. 9 between locations 3 and 4) likely driven by radiative heating. The rest of the frozen and buried lake (Fig. 9 between locations 1 and 3) has persistent accumulated snow insulating the ice underneath preventing the onset of melt. Landsat ETM+ images during the peak of the 2011 melt season (Fig. 10) demonstrate that lake extent corresponds to regions in the radar echogram where melt was initiated (Fig. 10 between locations 3 to 4) and that the region of the buried lake maintained a floating ice cap into the melt season (Fig. 10 between locations 2 to 3).

MODIS LST data, the only temperature data for this site and date, show a peak temperature of −10.7 °C during the 16:40 GMT overpass. Radar and DMS data were acquired over this site at 16:09 GMT very close to peak temperature and solar input. MODIS LST is rather low for the production of water observed in the echogram over this site which is probably the result of the relatively coarse spatial resolution (1 km) of MODIS such that the very small patch of surface melt, or melt from a few cm below the surface, at the edge of the lake was not resolved. This indicates that the early onset of melt is spatially heterogeneous primarily occurring at locations where darker ice is exposed and that some of the first melt of the season is associated with exposed buried lakes.

5.3 Depth distribution of buried lakes

Figure 11 shows a histogram of the digitized water layer depths from every radar return over a buried lake. The average buried lake depth during the April and May OIB flights of 2011 was 4.20 + 0.42 m with a total range of 0.35 + 0.04 m to 25.48 + 2.55 m and a standard deviation of 3.18 m. There is not a distinctive pattern in buried lake depths along the margins of the GrIS. 38 % of radar returns delineated a snow layer above the lake ice with an average snow layer thickness over the buried lakes of 1.17 m (range of 0.31 m to 4.7 m) and an average ice layer thickness of 2.96 m (range of 1.01 m to 11.41 m). Uncertainties associated with estimates of density stratigraphy across the GrIS, which is used to convert radar travel time to depth, likely cause a shallow bias in these depth measurements of on average 10 % and up to 22 %. Nonetheless, our estimates provide the first initial determination of the depth of stored water in buried lakes below the surface of the GrIS as well as constrain the thickness of lake ice that forms over the buried lakes.

6 Results

Though the water stored in buried lakes is spatially extensive it is a very small amount of mass that likely has little influence on mass loss projections for Greenland. Assuming all the buried lakes detected in 2011, the year with the maximum number of lakes, were the size of the mean supraglacial lake detected by Selmes et al. (2011) with a large water depth of 10 m, the volume of water retained in the lakes would amount to ~ 1.5 Gt of water over an area of $\sim 140\,\mathrm{km}^2$. For comparison the englacial storage of water in the firn aquifer, recently discovered in Southeast, Greenland covers an area of $\sim 70\,000\,\mathrm{km}^2$ with ~ 140 Gt of stored englacial water (Forster et al., 2013; Koenig et al., 2014). While the amount of water stored is likely insignificant, the spatial distribution of the retained water is certainly locally important for the development of the englacial hydrologic network and glacial dynamics.

6.1 Buried lakes and drainage behavior

Stored meltwater in buried lakes during the winter can have a significant effect on the drainage dynamics of supraglacial lakes. Drainage through hydro-fracture can occur if three primary criteria are met: (1) local tensile stress at the tip of an initial crack must exceed the critical stress intensity, (2) once a fracture has been initiated, crack propagation is facilitated by a steady supply of meltwater keeping the fracture water-filled and (3) meltwater influx must be sufficient to overcome refreezing (van der Veen et al., 1998; Alley et al., 2005; van der Veen, 2007). Buried meltwater likely has the most impact on both fracture re-initialization as the melt season advances and the lake basin fracture system becomes activated. Given the volumetric rate of freezing within a crack integrated over a given depth is partially a function of the difference between the water temperature and ice temperature (Alley et al., 2005), resident meltwater stored at depth would have to arrive at an equilibrium temperature over the winter resulting in some refreezing and latent heat added to the fracture walls. This would raise the ice temperature likely making it easier to activate the conduit in the spring/summer. Over successive seasons, supraglacial lakes that become buried lakes in the wintertime may drain more readily. What is still not well understood are the mechanisms that result in trapping meltwater at depth, particularly over several seasons. Initial results from this analysis over a sample lake with a surface expression indicate that the buried lakes may control the summertime lake surface extent. These relationships are not well understood. Additional work is necessary to understand the role that seasonal accumulation as well as post-drainage processes (refreezing, incomplete drainage, and creep closure at depth) play in supporting the formation of buried lakes.

6.2 Implications for ice dynamics and hydrology

The retained water in buried lakes will locally warm ice at the surface of the ice sheet as measured and modeled by Humphreys et al. (2012) and Kuiper Munneke et al. (2014). Additionally the buried lake water, as explained previously, can initiate cracks or fractures, delivering meltwater, and its associated latent heating, deeper into the ice sheet. The resultant heating and softening of the ice could affect ice flow dynamics, especially if concentrations of buried lakes are located at lateral margins of outlet glaciers.

Buried lakes provide a possible water source for the peaks in stream discharge observed by Rennermalm et al. (2013) when no surface melt was present. As explained previously, it is expected that regions with high concentrations of buried lakes would eventually lead to areas with more developed englacial pathways due to the year-round pressure from the retained water. Additionally, buried lakes represent a year-round source of water that could drain anytime routing water through any open englacial conduits.

When buried lakes thaw in the summer it is expected that they would initially contain a larger amount of water than neighboring refrozen or drained lakes. In the fall, as the lakes begin to freeze, it is expected the buried lakes would be relatively larger and either contain more water or contain more insulated water beneath ice cover. The expected initial positive water budget at the start of the melt season for a given lake basin that contains buried lakes may also be an important driver for the development of supraglacial channels. As meltwater runoff fills a basin the total storage capacity will more likely be exceeded if water is already present. Therefore, buried lakes may be an initial condition for the initiation and evolution of supraglacial channels. This is especially important for channels that are most efficient at transporting runoff into moulins, which provide large and rapid meltwater access to the bedrock. Additional work is necessary to evaluate the role buried water may play in these supraglacial hydrologic systems.

How and which supraglacial lakes become buried lakes, is still unanswered. Analyzing MODIS, Landsat and other moderate to high resolution surface imagery is necessary to determine the spatial and depth evolution of supraglacial lakes to determine the processes and characteristics that define which lakes drain rapidly, drain slowly, refreeze or become buried lakes. Additionally, the short times series of this data as well as the temporally changing flight lines make it impossible to determine if the amount of water stored over the winter is increasing. With increasing melt extent across the GrIS (Mote et al., 2007; Nghiem et al., 2012; Hall et al., 2013) it is hypothesized that water storage in buried lakes may also be increasing, especially at higher elevations on the

TCD
8, 3999–4031, 2014

ice sheet. Previous and on-going satellite radar sensors, such as RADARSAT, ERS-1 and -2, OSCAT and ASCAT, may be able to detect the buried lakes and provide a better spatial and temporal time series to analyze trends. These investigations will be left for future research.

7 Conclusions

Buried lakes are extensively distributed around the margins of the GrIS. A few previous studies suggested that water remained in the supraglacial lakes late into the winter season; however, these data are the first to confirm and extensively map the distribution of the retained water. Though the water retained in buried lakes is insignificant compared to total mass loss, it has important implications for the local temperature profile, development of the englacial hydrologic network and ice dynamics. This research presents a new understanding of meltwater routing through and within the GrIS and emphasizes the need to better understand the hydrologic pathways through which meltwater drains toward the ocean. Ultimately, understanding surface melt and supraglacial lake water storage and drainage will lead to a better understanding of how the increases in the GrIS mass loss from surface melt contribute to SLR over time.

Acknowledgements. The authors thank L. Brucker and T. Neumann for their insightful discussions. This work was supported by the NASA's New Investigator and Cryospheric Sciences Programs. Data collection and instrument development were made possible by The University of Kansas' Center for Remote Sensing of Ice Sheets (CReSIS) supported by the National Science Foundation and Operation IceBridge. S.E.M supported by NASA's Earth and Space Science Fellowship Program grant NNX12AN98H.

References

Alley, R. B., Dupont, T. K., Parizek, B. R., and Anandakrishnan, S.: Access of surface meltwater to beds of sub-freezing glaciers: preliminary insights, Ann. Glaciol., 40, 8–14, 2005.

Bartholomew, I., Nienow, P., Sole, A., Mair, D., Cowton, T., Palmer, S., and Wadham, J.: Supraglacial forcing of subglacial drainage in the ablation zone of the Greenland ice sheet, Geophys. Res. Lett., 38, L08502, doi:10.1029/2011GL047063, 2011.

Benson, C. S.: Stratiraphic studies in the snow and firn of the Greenland Ice sheet, SIPRE Res. Rep., US Army Corps of Engineers, 70, 1962.

Box, J. E. and Ski, K.: Remote sounding of Greenland supraglacial melt lakes: implications for subglacial hydraulics, J. Glaciol., 53, 257–265, doi:10.3189/172756507782202883, 2007.

Catania, G. A., Neumann, T. A., and Price, S. F.: Characterizing englacial drainage in the ablation zone of the Greenland ice sheet, J. Glaciol., 54, 567–578, doi:10.3189/002214308786570854, 2008.

Comiso, J. C.: Warming trends in the Arctic from clear sky satellite observations, J. Climate, 16, 3498–3510, doi:10.1175/1520-0442(2003)016<3498:WTITAF>2.0.CO;2, 2003.

Das, S. B., Joughin, I., Behn, M. D., Howat, I. M., King, M. A., Lizarralde, D., and Bhatia, M. P.: Fracture propagation to the base of the Greenland Ice Sheet during supraglacial lake drainage, Science, 320, 778–781, doi:10.1126/science.1153360, 2008.

Dominguez, R.: IceBridge DMS L1B Geolocated and Orthorectified Images, NASA DAAC at the National Snow and Ice Data Center, Boulder, Colorado, 2014.

Dowdeswell, J. A. and Evans, S.: Investigations of the form and flow of ice sheets and glaciers using radio-echo sounding, Rep. Prog. Phys., 67, 1821–1861, doi:10.1088/0034-4885/67/10/R03, 2004.

Echelmeyer, K., Clarke, T. S., and Harrison, W. D.: Surficial glaciology of Jakobshavns Isbrae, West Greenland 1. Surface-morphology, J. Glaciol., 37, 368–382, 1991.

Forster, R. R., Box, J. E., van den Broeke, M. R., Miège, C., Burgess, E. W., van Angelen, J. H., Lenaerts, J. T. M., Koenig, L. S., Paden, J., Lewis, C., Gogineni, S. P., Leuschen, C., and McConnell, J. R.: Extensive liquid meltwater storage in firn within the Greenland ice sheet, Nat. Geosci., 7, 95–98, doi:10.1038/ngeo2043, 2013.

Grenfell, T. C. and Perovich, D. K.: Radiation absorption-coefficients of polycrystalline ice from 400–1400 nm, J. Geophys. Res. Atmos., 86, 7447–7450, doi:10.1029/JC086iC08p07447, 1981.

Hall, D. K., Box, J. E., Casey, K. A., Hook, S. J., Shuman, C. A., and Steffen, K.: Comparison of satellite-derived and in-situ observations of ice and snow surface temperatures over Greenland, Remote Sens. Environ., 112, 3739–3749, doi:10.1016/j.rse.2008.05.007, 2008.

Hanna, E., Fettweis, X., Mernild, S. H., Cappelen, J., Ribergaard, M. H., Shuman, C. A., Steffen, K., Wood, L., and Mote, T. L.: Atmospheric and oceanic climate forcing of the exceptional Greenland ice sheet surface melt in summer 2012, Int. J. Climatol., 34, 1022–1037, doi:10.1002/joc.3743, 2014.

Harper, J., Humphrey, N., Pfeffer, W. T., Brown, J., and Fettweis, X.: Greenland ice-sheet contribution to sea-level rise buffered by meltwater storage in firn, Nature, 491, 240–243, doi:10.1038/nature11566, 2012.

Hoffman, M. J., Catania, G. A., Neumann, T. A., Andrews, L. C., and Rumrill, J. A.: Links between acceleration, melting, and supraglacial lake drainage of the western Greenland Ice Sheet, J. Geophys. Res.-Earth, 116, F04035, doi:10.1029/2010JF001934, 2011.

Howat, I. M., de la Peña, S., van Angelen, J. H., Lenaerts, J. T. M., and van den Broeke, M. R.: *Brief Communication* "Expansion of meltwater lakes on the Greenland Ice Sheet", The Cryosphere, 7, 201–204, doi:10.5194/tc-7-201-2013, 2013.

Humphrey, N. F., Harper, J. T., and Pfeffer, W. T.: Thermal tracking of meltwater retention in Greenland's accumulation area, J. Geophys. Res., 117, F01010, doi:10.1029/2011JF002083, 2012.

Joughin, I., Das, S. B., King, M. a, Smith, B. E., Howat, I. M., and Moon, T.: Seasonal speedup along the western flank of the Greenland Ice Sheet, Science, 320, 781–783, doi:10.1126/science.1153288, 2008.

Koenig, L. S. and Hall, D. K.: Comparison of satellite, thermochron and air temperatures at Summit, Greenland, during the winter of 2008/09, J. Glaciol., 56, 735–741, 2010.

Koenig, L. S., Miège, C., Forster, R. R., and Brucker, L.: Initial in situ measurements of perennial meltwater storage in the Greenland firn aquifer, Geophys. Res. Lett., 41, 81–85, doi:10.1002/2013GL058083, 2014.

Krawczynski, M. J., Behn, M. D., Das, S. B., and Joughin, I.: Constraints on the lake volume required for hydro-fracture through ice sheets, Geophys. Res. Lett., 36, L10501, doi:10.1029/2008GL036765, 2009.

Lampkin, D. J.: Supraglacial lake spatial structure in western Greenland during the 2007 ablation season, J. Geophys. Res., 116, F04001, doi:10.1029/2010JF001725, 2011.

Langford, V. S., McKinley, A. J., and Quickenden, T. I.: Temperature dependence of the visible-near-infrared absorption spectrum of liquid water, J. Phys. Chem. A, 105, 8916–8921, doi:10.1021/jp010093m, 2001.

Leuschen, C.: IceBridge Snow Radar L1B Geolocated Radar Echo Strength Profiles, NASA DAAC at the National Snow and Ice Data Center, Boulder, Colorado, 2014.

Luck, W. A. P.: A model of hydrogen-bonded liquids, Angew. Chem. Int. Edit., 19, 28–41, 1980.

McMillan, M., Nienow, P., Shepherd, A., Benham, T., and Sole, A.: Seasonal evolution of supra-glacial lakes on the Greenland Ice Sheet, Earth Planet. Sc. Lett., 262, 484–492, doi:10.1016/j.epsl.2007.08.002, 2007.

Mote, T. L.: Greenland surface melt trends 1973–2007: Evidence of a large increase in 2007, Geophys. Res. Lett., 34, L22507, doi:10.1029/2007gl031976, 2007.

Munneke, P. K. M., Ligtenberg, S. R., van den Broeke, M. R., van Angelen, J. H., and Forster, R. R.: Explaining the presence of perennial liquid water bodies in the firn of the Greenland Ice Sheet, Geophys. Res. Lett., 41, 476–483, doi:10.1002/2013GL058389, 2014.

Nghiem, S. V., Hall, D. K., Mote, T. L., Tedesco, M., Albert, M. R., Keegan, K., Shuman, C. A., DiGirolamo, N. E., and Neumann, G.: The extreme melt across the Greenland ice sheet in 2012, Geophys. Res. Lett., 39, L20502, doi:10.1029/2012GL053611, 2012.

Ohmura, A., Steffen, K., Blatter, H., Greuell, W., Rotach, M., Konzelmann, T., Laternser, M., Ouchi, A., and Steiger, D.: Energy and mass balance during the melt season at the equilibrium line altitude, Paakitsoq, Greenland Ice Sheet, Progress Report No. 1, Eidgenoss. Tech. Hochschule, Department of Geography, Zurich, 1991.

Palmer, S., Shepherd, A., Nienow, P., and Joughin, I.: Seasonal speedup of the Greenland Ice Sheet linked to routing of surface water, Earth Planet. Sc. Lett., 302, 423–428, doi:10.1016/j.epsl.2010.12.037, 2011.

Panzer, B., Gomez-Garcia, D., Leuschen, C., Paden, J., Rodriguez-Morales, F., Patel, A., Markus, T., Holt, B., and Gogineni, P.: An ultra-wideband, microwave radar for measuring snow thickness on sea ice and mapping near-surface internal layers in polar firn, J. Glaciol., 59, 244–254, doi:10.3189/2013JoG12J128, 2013.

Rennermalm, A. K., Smith, L. C., Chu, V. W., Box, J. E., Forster, R. R., Van den Broeke, M. R., Van As, D., and Moustafa, S. E.: Evidence of meltwater retention within the Greenland ice sheet, The Cryosphere, 7, 1433–1445, doi:10.5194/tc-7-1433-2013, 2013.

Rodriguez-Morales, F., Gogineni, S., Leuschen, C. J., Paden, J. D., Li, J., Lewis, C. C., Panzer, B., Alvestegui, D. G.-G., Patel, A., Byers, K., Crowe, R., Player, K., Hale, R. D.,

Arnold, E. J., Smith, L., Gifford, C. M., Braaten, D., and Panton, C.: Advanced multifrequency radar instrumentation for polar research, IEEE T. Geosci. Remote, 52, 2824–2842, doi:10.1109/TGRS.2013.2266415, 2014.
Selmes, N., Murray, T., and James, T. D.: Fast draining lakes on the Greenland Ice Sheet, Geophys. Res. Lett., 38, L15501, doi:10.1029/2011GL047872, 2011.
Shepherd, A., Ivins, E. R., A, G., Barletta, V. R., Bentley, M. J., Bettadpur, S., Briggs, K. H., Bromwich, D. H., Forsberg, R., Galin, N., Horwath, M., Jacobs, S., Joughin, I., King, M. A., Lenaerts, J. T. M., Li, J., Ligtenberg, S. R. M., Luckman, A., Luthcke, S. B., McMillan, M., Meister, R., Milne, G., Mouginot, J., Muir, A., Nicolas, J. P., Paden, J., Payne, A. J., Pritchard, H., Rignot, E., Rott, H., Sørensen, L. S., Scambos, T. A., Scheuchl, B., Schrama, E. J. O., Smith, B., Sundal, A. V, van Angelen, J. H., van de Berg, W. J., van den Broeke, M. R., Vaughan, D. G., Velicogna, I., Wahr, J., Whitehouse, P. L., Wingham, D. J., Yi, D., Young, D., and Zwally, H. J.: A reconciled estimate of ice-sheet mass balance, Science, 338, 1183–1189, doi:10.1126/science.1228102, 2012.
Sneed, W. A. and Hamilton, G. S.: Validation of a method for determining the depth of glacial melt ponds using satellite imagery, Ann. Glaciol., 52, 15–22, 2011.
Sundal, A. V, Shepherd, A., Nienow, P., Hanna, E., Palmer, S., and Huybrechts, P.: Evolution of supra-glacial lakes across the Greenland Ice Sheet, Remote Sens. Environ., 113, 2164–2171, doi:10.1016/j.rse.2009.05.018, 2009.
Sundal, A. V., Shepherd, A., Nienow, P., Hanna, E., Palmer, S., and Huybrechts, P.: Melt-induced speed-up of Greenland ice sheet offset by efficient subglacial drainage, Nature, 469, 522–U83, doi:10.1038/nature09740, 2011.
Tedesco, M. and Steiner, N.: In-situ multispectral and bathymetric measurements over a supraglacial lake in western Greenland using a remotely controlled watercraft, The Cryosphere, 5, 445–452, doi:10.5194/tc-5-445-2011, 2011.
Tedstone, A. J., Nienow, P. W., Sole, A. J., Mair, D. W. F., Cowton, T. R., Bartholomew, I. D., and King, M. A.: Greenland ice sheet motion insensitive to exceptional meltwater forcing, P. Natl. Acad. Sci. USA, 110, 19719–19724, doi:10.1073/pnas.1315843110, 2013.
Ulaby, F. T., Moore, R. K., and Fung, A. K.: Microwave Remote Sensing: Active and Passive, vol. 2, Advanced Book Program/World Science Division, Addison-Wesley Pub. Co., Reading, Mass., 1981.

TCD
8, 3999–4031, 2014

Van den Broeke, M., Bamber, J., Ettema, J., Rignot, E., Schrama, E., van de Berg, W. J., van Meijgaard, E., Velicogna, I., and Wouters, B.: Partitioning recent Greenland mass loss, Science, 326, 984–986, doi:10.1126/science.1178176, 2009.

Van der Veen, C. J.: Fracture propagation as means of rapidly transferring surface meltwater to the base of glaciers, Geophys. Res. Lett., 34, L01501, doi:10.1029/2006GL028385, 2007.

Van der Veen, C. J., Krabill, W. B., Csatho, B. M., and Bolzan, J. F.: Surface roughness on the Greenland ice sheet from airborne laser altimetry, Geophys. Res. Lett., 25, 3887–3890, doi:10.1029/1998GL900041, 1998.

Vernon, C. L., Bamber, J. L., Box, J. E., van den Broeke, M. R., Fettweis, X., Hanna, E., and Huybrechts, P.: Surface mass balance model intercomparison for the Greenland ice sheet, The Cryosphere, 7, 599–614, doi:10.5194/tc-7-599-2013, 2013.

Wan, Z. M., Zhang, Y. L., Zhang, Q. C., and Li, Z. L.: Validation of the land-surface temperature products retrieved from Terra Moderate Resolution Imaging Spectroradiometer data, Remote Sens. Environ., 83, 163–180, 2002.

Warren, S. G.: Optical-constants of ice from the ultraviolet to the microwave, Appl. Optics, 23, 1206–1225, 1984.

Wiesmann, A. and Matzler, C.: Microwave emission model of layered snowpacks, Remote Sens. Environ., 70, 307–316, doi:10.1016/S0034-4257(99)00046-2, 1999.

Zwally, H. J., Abdalati, W., Herring, T., Larson, K., Saba, J., and Steffen, K.: Surface melt-induced acceleration of Greenland ice-sheet flow, Science, 297, 218–222, doi:10.1126/science.1072708, 2002.

Table 1. Number of buried lakes detected in each year along with the OIB flight line distance flown below 2000 m, the mean elevation and standard deviation of lake elevations and the number of buried lake below 1000 m in elevation. See Fig. 6 for spatial distribution.

Year Collected	# Buried Lakes Detected	Flightlines below 2000 m (km)	Mean Elevation (m)	Std Elevation	Buried Lakes below 1000 m
2009	57	26 937	1268	290	8
2010	85	39 246	1180	399	28
2011	174	44 503	1415	295	18
2012	127	41 276	1371	332	19

TCD
8, 3999–4031, 2014

Table 2. Number of multi-year buried lakes detected over two and three years. See Fig. 7 for spatial distribution.

	2010	2011	2012
2009	9	10	7
2010		5	7
2011			15

TCD
8, 3999–4031, 2014

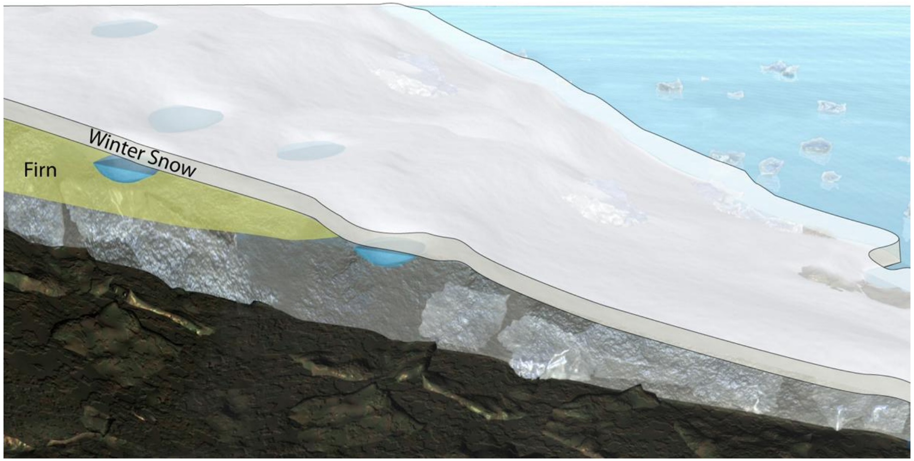

Figure 1. An early spring cross section illustration of buried supraglacial lakes (blue) still filled with water after the winter season.

TCD
8, 3999–4031, 2014

Wintertime storage of water in buried supraglacial lakes across the GrIS

L. S. Koenig et al.

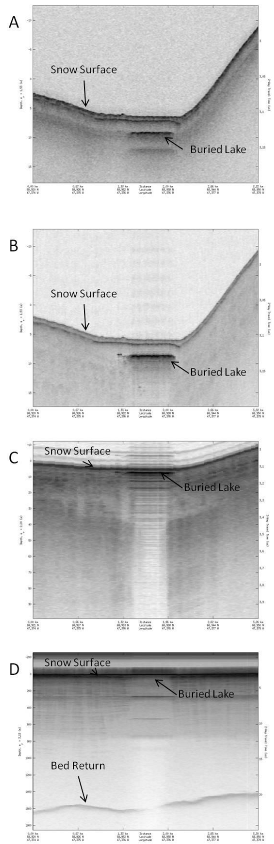

Figure 2. Radar echograms from Western Greenland (∼ 90 km inland of Jakoshavn's terminus) showing radar signal attenuation at multiple frequencies over a buried lake from the **(A)** Ku-band Radar (∼ 13–17 GHz) **(B)** Snow Radar (∼ 2–6 GHz) **(C)** Accumulation Radar (∼ 600–900 MHz) and **(D)** MCoRDS Radar (∼ 140–260 MHz).

TCD
8, 3999–4031, 2014

Wintertime storage of water in buried supraglacial lakes across the GrIS

L. S. Koenig et al.

Title Page
Abstract | Introduction
Conclusions | References
Tables | Figures
◀| |▶
◀ ▶
Back | Close
Full Screen / Esc
Printer-friendly Version
Interactive Discussion

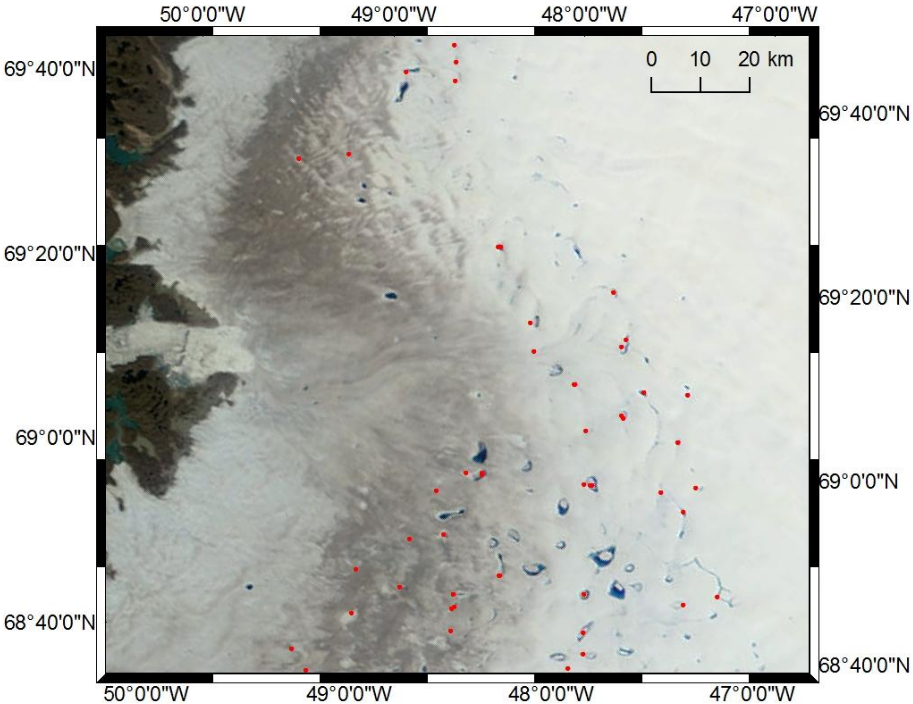

Figure 3. MODIS Rapid Response image from 7 August 2010 with buried lake detections from April–May 2011 (red dots) overlying many of the supraglacial lakes.

TCD
8, 3999–4031, 2014

Wintertime storage of water in buried supraglacial lakes across the GrIS

L. S. Koenig et al.

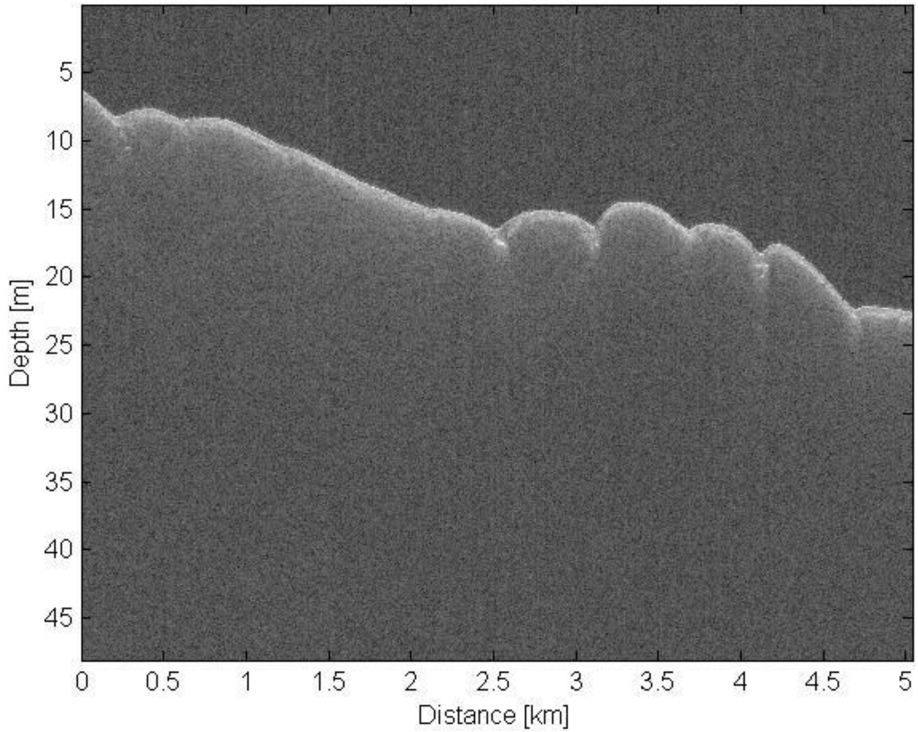

Figure 4. Snow Radar echogram likely showing a water filled crevasse field which was not included in the buried lakes mapping.

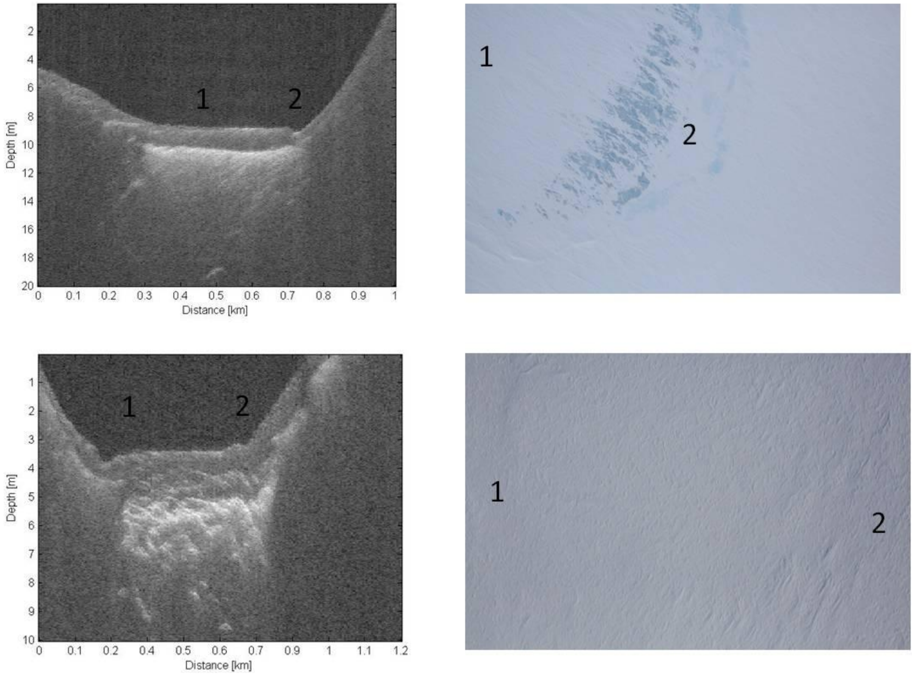

Figure 5. Snow Radar echogram of buried lakes (left) with DMS imagery of the GrIS surface (right) from: (top) a rare buried lake in Northwest Greenland (~ 45 km inland from the terminus of Streenstrup Glacier) with a surface expression showing darker blue where there is buried liquid water and a more turquoise, lighter blue where the lake is frozen through and (bottom) a typical buried lake in Western Greenland (~ 60 km inland from the terminus of Jakobsavn Isbrae) showing surface sastrugi and no detectable lake surface expression.

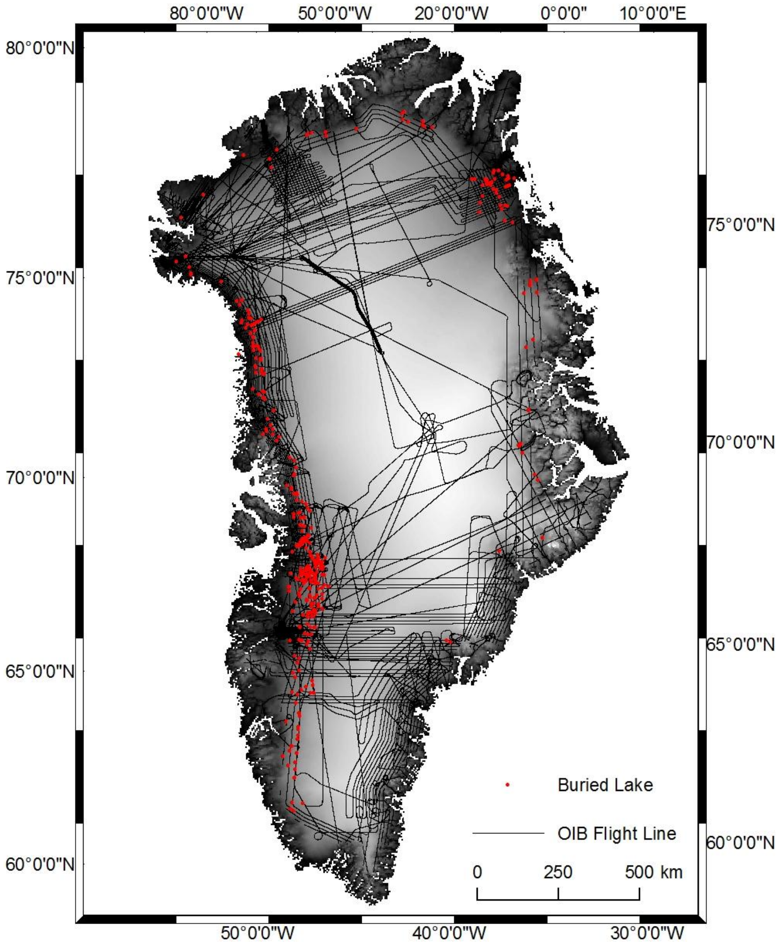

Figure 6. Locations of buried lakes (red circles) from 2009–2012 with OIB flight lines (black lines).

TCD
8, 3999–4031, 2014

Wintertime storage of water in buried supraglacial lakes across the GrIS

L. S. Koenig et al.

Title Page
Abstract
Introduction
Conclusions
References
Tables
Figures
◀
▶
Back
Close
Full Screen / Esc
Printer-friendly Version
Interactive Discussion

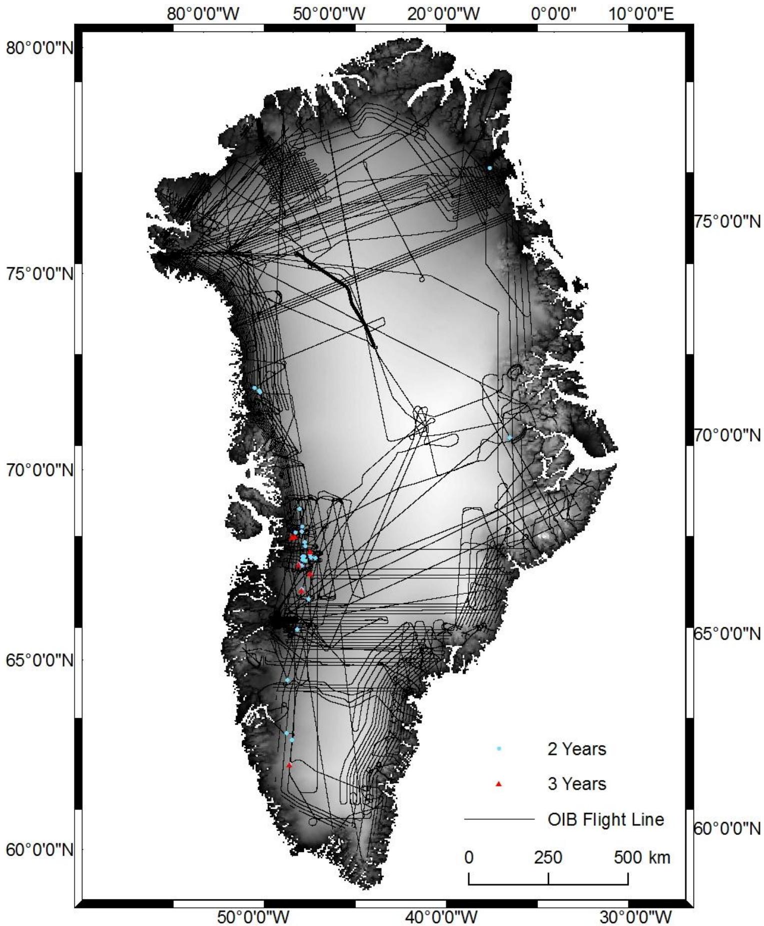

Figure 7. Locations of multi-year buried lakes detected in 2 years (blue circles) and 3 years (red triangles) from 2009–2012 with OIB flight lines (black lines).

TCD
8, 3999–4031, 2014

Wintertime storage of water in buried supraglacial lakes across the GrIS

L. S. Koenig et al.

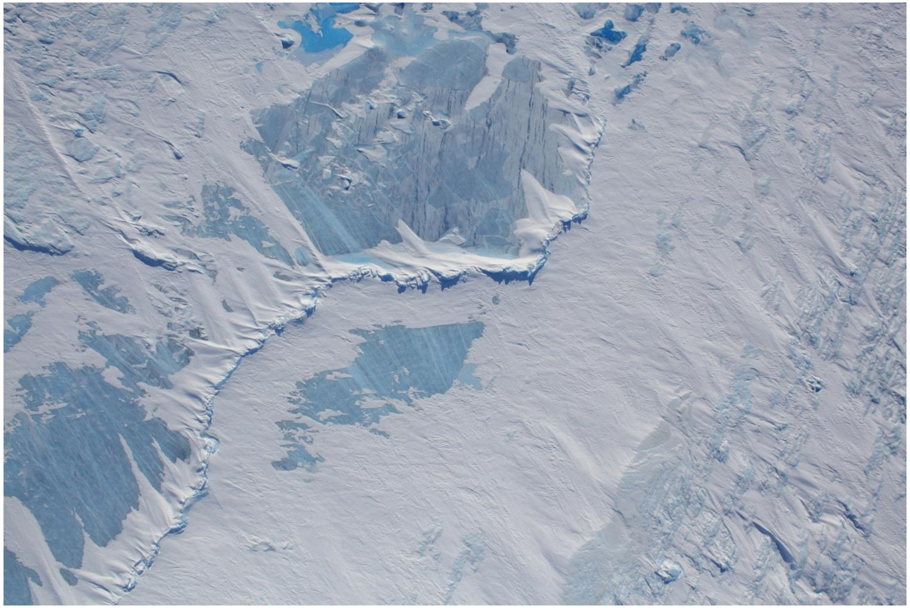

Figure 8. DMS image from 2 May 2011 of a buried lake with a surface expression showing snow blowing across the clear frozen surface of the lake, water filled cracks at the bottom of the lake, a pressure ridge likely caused by the retained water and the characteristic darker blue color where there is retained water and a turquoise blue color on the frozen edges of the lake.

TCD
8, 3999–4031, 2014

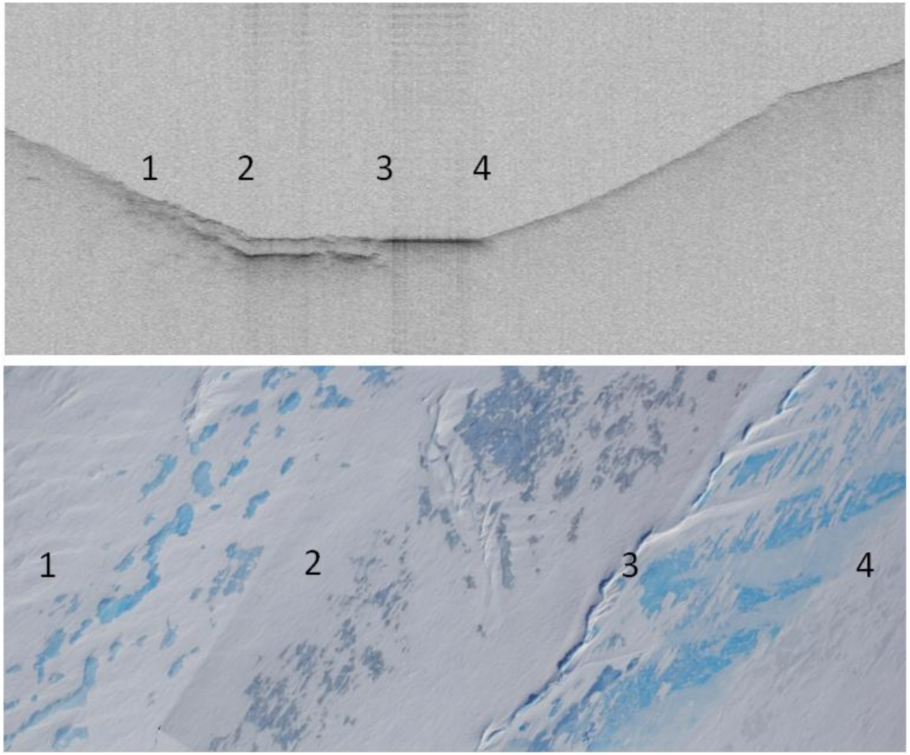

Figure 9. Snow Radar echogram (top) with DMS image of GrIS snow surface (bottom) taken on 2 May 2011 for a buried lake in North Greenland (~ 100 km inland from the terminus Zashariae Isstrøm Glacier) showing from location 1 to 2 the turquoise blue refrozen lake, from 2 to 3 the darker blue retained water, a pressure ridge at 3, and from 3 to 4 surface melt caused by radiative heating at the surface of the refrozen lake edge.

TCD
8, 3999–4031, 2014

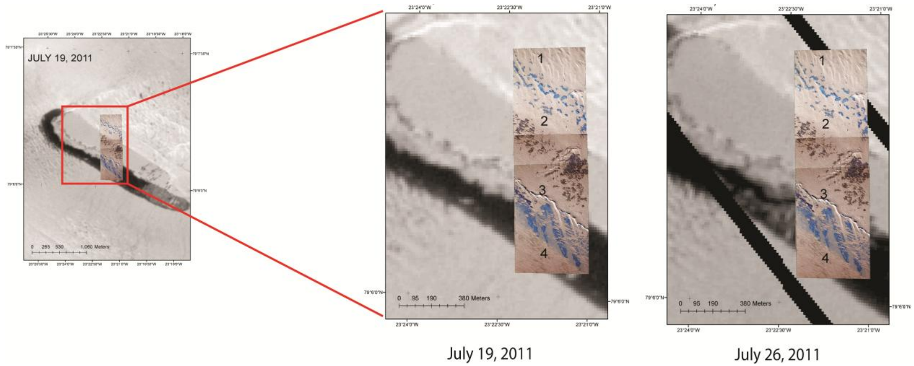

Figure 10. DMS image for the buried lake in Fig. 9 superimposed over a Landsat ETM+ image acquired on 19 July 2011. Expanded images are of the same location over the section of the lake where the DMS image covers for both 19 and 26 July 2011. These images correlate the boundaries of the initial melt with the lake extent observed later that summer (3 to 4) and that the stored water (2–3) maintained a floating ice cap through the summer.

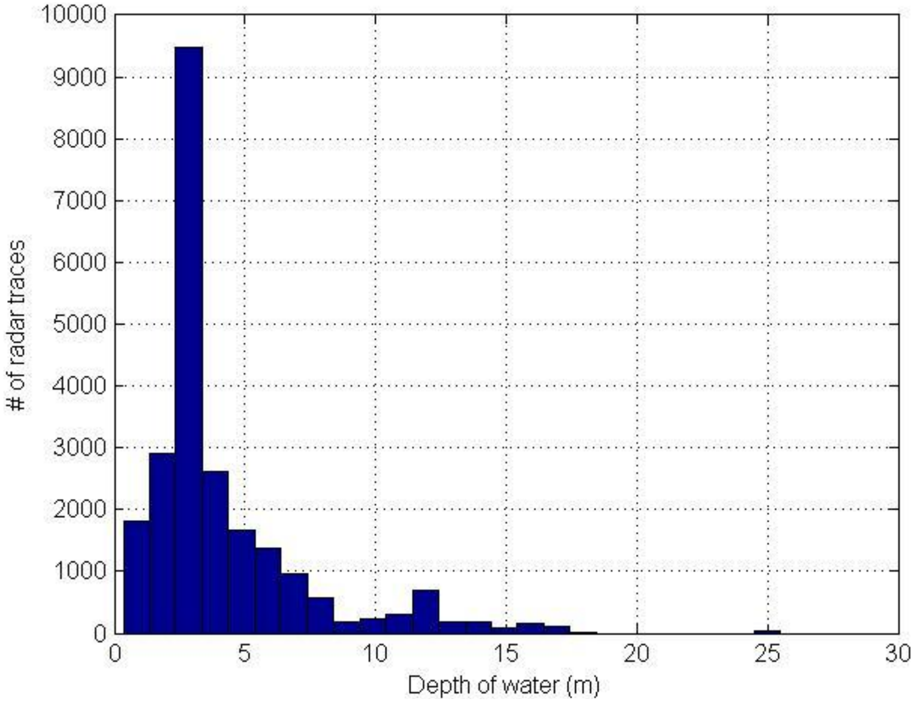

Figure 11. Histogram showing the depth of the water surface from every radar return over a buried lake. Error estimates on the depth are on average 10 % shallower due to uncertainties associated with the stratigraphy of density across the GrIS, which is used to convert radar travel time to depth.